Acta Crystallographica Section D
Biological Crystallography
ISSN 0907-4449

addenda and errata

Structure of the saccharide-binding domain of the human natural killer cell inhibitory receptor p75/AIRM1. Erratum

Nazzareno Dimasi,[a]* Helen Attrill,[b,c] Daan M. F. van Aalten,[c] Alessandro Moretta,[d,e] Lorenzo Moretta,[a,e] Roberto Biassoni[a] and Roy A. Mariuzza[f]

[a]Istituto Giannina Gaslini, Largo Gerolamo Gaslini 5, 16147 Genova, Italy, [b]Division of Cell Biology and Immunology, School of Life Sciences, University of Dundee, Dundee DD1 5EH, Scotland, [c]Division of Biological Chemistry and Molecular Microbiology, School of Life Sciences, University of Dundee, Dundee DD1 5EH, Scotland, [d]Dipartimento di Medicina Sperimentale, Sezione di Istologia, Via Marsano 10, Università di Genova,Italy, [e]Dipartimento di Medicina Sperimentale, Sezione Patalogia Gernerale, Via Alberti 2, Università di Genova,Italy, and [f]Center for Advanced Research in Biotechnology, W. M. Keck Laboratory for Structural Biology, University of Maryland Biotechnology Institute, 9600 Gudelsky Drive, Rockville, Maryland 2085, USA. Correspondence e-mail: ndimasi@email.it

In the paper by Dimasi *et al.* [(2004), *Acta Cryst.* D**60**, 401–403] two authors were not included. The correct list of authors is given above. It should also be noted that Nazzareno Dimasi and Helen Attrill contributed equally to the work described in the paper, and the following acknowledgent also applies to the paper.

This work was supported by NIH grant AI47990 to RAM and BBSRC Grant 94/B14010 to DMFvA and by a Wellcome Trust Career Development Research Fellowship to DMFvA. Financial support was also provided by AIRC, Progetto Stategico 2002 Ministero della Salute and CNR Functional Genomics to RB. ND would like to thank Ministero Italiano della Salute for providing financial support.

References

Dimasi, N., Moretta, A., Moretta, L., Biassoni, R. & Mariuzza, R. (2004). *Acta Cryst.* D**60**, 401–403.

  DOI: 10.1107/S0907444904002951

Acta Crystallographica Section D
Biological Crystallography
ISSN 0907-4449

Structure of the hybrid cluster protein (HCP) from *Desulfovibrio desulfuricans* ATCC 27774 containing molecules in the oxidized and reduced states

Sofia Macedo,[a,b] David Aragão,[a,b] Edward P. Mitchell[b] and Peter Lindley[a,b]*

[a]Instituto de Tecnologia Química e Biológica, Universidade Nova de Lisboa, Av. República, EAN, Apartado 127, 2781-901 Oeiras, Portugal, and [b]European Synchrotron Radiation Facility, BP-220, F-38043 Grenoble CEDEX, France

Correspondence e-mail: lindley@itqb.unl.pt

Received 12 September 2003
Accepted 4 November 2003

PDB Reference: hybrid cluster protein, 1upx, r1upxsf.

The hybrid cluster protein (HCP) from the sulfate-reducing bacteria *Desulfovibrio desulfuricans* ATCC 27774 has been isolated and crystallized anaerobically. The protein sample used in the crystallization studies was several months old, having been stored at 193 K, and initial crystal structure studies were unable to fully resolve details of the hybrid cluster despite the use of high-resolution data to 1.25 Å collected at the ESRF, Grenoble, France. Full elucidation of the structure has only become possible with the complete knowledge of the as-isolated and fully reduced crystal structures. The analysis clarifies the significant movements in the position of the Fe atom linked to the persulfide moiety in the oxidized as-isolated protein and the S atom of the persulfide itself as the protein is reduced. The structures of the as-isolated and reduced states are discussed in terms of the putative function of the HCP proteins.

1. Introduction

Hybrid cluster proteins (HCPs; formerly known as prismanes) are encoded by genes in a large number of prokaryotes, including archaea and bacteria, both strictly anaerobic and facultative anaerobic, as well as in eukaryotic protozoa. However, despite a wealth of biochemical, spectroscopic and high-resolution X-ray structural information, no specific function has yet been assigned to this family of proteins. Involvement in the biological nitrogen cycle has been proposed (van den Berg *et al.*, 2000; Beliaev *et al.*, 2002; Wolfe *et al.*, 2002), as well as an adaptive response to oxidative stress (Briolat & Reysset, 2002). The similarity of the hybrid Fe—S cluster in HCPs to the nickel-containing cluster present in the catalytic domain of the carbon monoxide dehydrogenase from *Carboxydothermus hydrogenoformans* has also been noted (Dobbek *et al.*, 2001; Macedo *et al.*, 2002). In a recent study, Kim *et al.* (2003) studied the modulation of virulence by two acidified nitrite-responsive loci of *Salmonella enterica* serovar *Typhimurium*. These authors note that the nitrite-inducible promoters are located upstream of loci designated *nipAB* and *nipC* which correspond to *hcp-hcr* (hybrid cluster protein) of *Escherichia coli* and *norA* of *Alcaligenes eutrophus*, respectively. Such a study refocuses attention on a putative role for the HCP in the nitrogen cycle.

After the initial discovery of the hybrid cluster (Arendsen *et al.*, 1998), some debate arose as to whether the structure was really an artifact resulting from the aerobic preparation and crystallization. This debate occurred despite considerable spectroscopic and biochemical evidence to suggest that the

Table 1
Data-collection statistics.

Values in parentheses refer to the highest resolution shell collected, 1.19–1.15 Å.

Beamline	ID14-2, ESRF
Space group	*P*1
Z	2
Resolution (Å)	
Crystal 1	30.0–1.40
Crystal 2	6.0–1.15
Wavelength (Å)	0.933
Unit-cell parameters	
a (Å)	57.30
b (Å)	61.20
c (Å)	72.00
α (°)	82.80
β (°)	73.70
γ (°)	87.30
No. of batches/rotation angle (°)	
Crystal 1	280/0.75
Crystal 2	244/0.5
No. of unique reflections	
Crystal 1	157207
Crystal 2	232683
Merged data from crystals 1 and 2	
No. of unique reflections to 1.15 Å resolution	280898
Average multiplicity	2.3 (1.3)
$R_{\rm merge}$†	0.082 (0.271)
Average $I/\sigma(I)$	3.6 (1.3)
Completeness (%)	84.8 (70.0)
Average *B* (Wilson) (Å$^{2)}$	6.0

† $R_{\rm merge} = \sum|I - \langle I\rangle|/\sum\langle I\rangle$.

as-isolated form of the protein was independent of the aerobic or anaerobic conditions used in its preparation. In order to unequivocally resolve the debate, it was decided to isolate, purify and crystallize the protein from *Desulfovibrio desulfuricans* ATCC 27774 (*Dd*) under strict anaerobic conditions. This was eventually achieved using fresh samples of the protein isolated at the ITQB in Portugal (Macedo *et al.*, 2002). However, in some early attempts using protein which had been prepared by the late Jean LeGall and his colleagues (University of Georgia, Athens, USA), transferred to the ITQB and kept in a freezer for several months at around 193 K, crystals were produced containing a structure that could not be fully interpreted. It was suspected that the crystals contained the structure of the as-isolated oxidized form of the protein, but heavily contaminated with another form. Only in the full light of the as-isolated oxidized (Macedo *et al.*, 2002) and dithionite-reduced (Aragão *et al.*, 2003) forms of the protein has it been possible to interpret the electron density resulting from data collected to high resolution on the old anaerobically treated protein sample. The present paper reports the X-ray crystal structure of the HCP from *Dd* containing both the oxidized and reduced forms of the protein.

2. Materials and methods

2.1. Crystallization

The sample of HCP from *Dd* was anaerobically purified by the late Jean LeGall and colleagues at the University of Georgia, USA in a similar manner to that previously described (Macedo *et al.*, 2002), transferred to the ITQB, Portugal and kept at around 193 K for several months before use. The crystals were grown in a nitrogen environment inside a glove-box system ($p_{\rm O_2} < 1$ p.p.m.) using the sitting-drop vapour-diffusion method. The pale yellow plate-like crystals grew at 279 K in 25% PEG 8000 and 0.1 *M* MES buffer pH 6.0. 1.5 µl protein solution (12.6 mg ml^{-1} in 20 m*M* Tris–HCl pH 7.6 and 0.2 *M* NaCl) and an equal amount of precipitant solution were allowed to equilibrate against 500 µl of the latter in the reservoir. Crystals took some 4–5 weeks to grow and reached maximum dimensions of approximately 0.2 × 0.1 × 0.08 mm. Crystals for diffraction experiments were then mounted in loops and frozen at 100 K within the anaerobic environment of the glove box and transferred to the synchrotron in a nitrogen Dewar. Crystals were also obtained with 25% PEG 4000, 0.1 *M* HEPES pH 7.0 with 0.2 *M* calcium acetate, but these gave very poor unusable diffraction patterns.

2.2. X-ray data collection

X-ray data were collected from two crystals on beamline ID14-2 at the ESRF synchrotron-radiation source, Grenoble, France using a wavelength of 0.933 Å. For the first crystal, the ADSC CCD detector was positioned at a distance of 135 mm from the sample in order to collect data between 30.0 and 1.4 Å resolution. The beam size used was 50 × 50 µm, with an oscillation range of 0.75° and four passes per frame with a frame exposure time of 2 s. For the second crystal, the detector was positioned 60 mm from the sample with a potential data-collection range down to 0.97 Å resolution. The beam size was chosen as 65 × 65 µm, with an oscillation range of 0.5° using one pass and 10 s exposure per frame.

Data for both crystals were processed using *DENZO* (Otwinowski & Minor, 1997). The program *SCALEIT* was used to check that the crystals were isomorphous and 280 batches from the first crystal were then merged with 244 batches from the second using *SCALA*; the indexed intensities were converted to structure factors using the program *TRUNCATE*. *SCALEIT*, *SCALA* and *TRUNCATE* are part of the *CCP*4 program suite (Collaborative Computational Project, Number 4, 1994). Details of the data collection are given in Table 1. In hindsight, it is clear that the data-collection strategy adopted was not the optimum, but lack of crystals and accessibility to the synchrotron prevented remedial actions. As a consequence, it was decided that because of the high values of $R_{\rm sym}$ and the overall weakness and low multiplicity of the high-resolution data, further work would proceed with data only to 1.25 Å resolution; the $R_{\rm sym}$ in the resolution range 1.29–1.25 Å is 24.1%. The data used comprised 227 130 unique reflections, corresponding to an overall completeness of 88.9%.

The asymmetric unit (equivalent to the unit cell for space group *P*1) accommodates two molecules of molecular weight 60 kDa, corresponding to a $V_{\rm M}$ of 2.03 Å^3 Da^{-1} (Matthews, 1968) and a solvent content of some 39%.

2.3. Structure solution and refinement

The structure was elucidated by the method of molecular replacement using the program *AMoRe* (Navaza, 1993) in a similar manner to that used for the anaerobically isolated oxidized structure (Macedo *et al.*, 2002). The starting model was the as-isolated oxidized structure of the HCP from *D. vulgaris* strain Hildenborough (*Dv*) (Arendsen *et al.*, 1998) from which the two Fe–S clusters and the solvent molecules had been removed; the *Dd* and *Dv* proteins share 64% sequence identity and differences were not considered at this stage. *AMoRe* enabled the location of both molecules in the asymmetric unit and solvent modification was then performed using *DM* (Cowtan & Main, 1998); the *R* factor and correlation coefficients were 43.1% and 44.2, respectively. The initial Fourier map was of high quality and clearly showed electron density consistent with the two molecules of the *Dd* protein in the asymmetric unit. In each molecule, nearly all the main-chain and many side-chain residues for *Dd* could be positioned directly. However, in the hybrid clusters the electron density could not be explained by the presence of the as-isolated oxidized form of the protein alone. Extra density was particularly evident in the vicinity of Fe8 and near to the moiety bridging Fe5 and Fe7 and assigned as an O atom (OH^- or water) on the basis of resonance Raman spectroscopy (de Vocht *et al.*, 1996). Fig. 1 shows part of the electron density at the hybrid cluster in molecule *A* and, superimposed, the as-isolated oxidized form of the HCP from *Dd*. However, when the structure of the reduced form of the protein became available (Aragão *et al.*, 2003) it was clear that the key features of the extra density could be matched well with the reduced form. A consideration of the respective peak volumes suggested a 2:1 ratio of the reduced and oxidized forms, respectively.

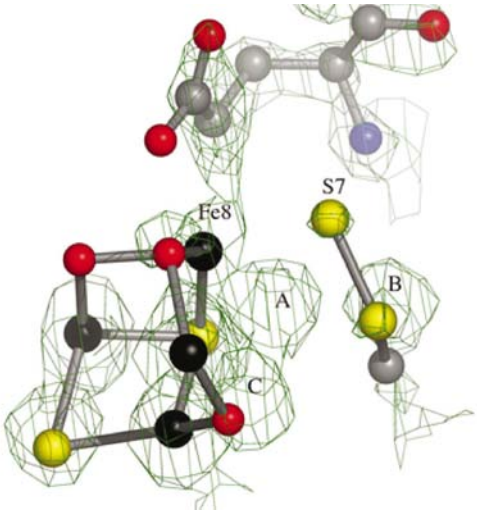

Figure 1
The $|F_o| - |F_c|$ electron-density synthesis at the hybrid cluster in molecule *A* prior to the refinement stage. At this time only the as-isolated oxidized form of the HCPs was known (Macedo *et al.*, 2002) and the superposition of this structure on the electron density clearly highlights many unexplained features including the maxima at A, B and C. After the elucidation of the reduced structure (Aragão *et al.*, 2003) it was possible to account for most of the additional density. Thus, the peaks labelled A, B and C are occupied by Fe8, the SG of Cys399 and S7 (part of the persulfide moiety in the oxidized form) in the reduced structure, respectively. The contour level is +3.0 r.m.s.

Refinement was performed using the maximum-likelihood functions implemented in *REFMAC* (Murshudov *et al.*, 1997). Rounds of conjugate-gradient sparse-matrix refinement with bulk-solvent modelling according to the Babinet principle (Tronrud, 1996) were alternated with model building using the *O* program (Jones *et al.*, 1991) in combination with σ_A-weighted $2|F_o| - |F_c|$ and $|F_o| - |F_c|$ electron-density maps (Read, 1986). For the hybrid clusters, only Fe5, Fe6, Fe7, S5 and S6 of the reduced form were initially included with full occupancy to give values of *R* and $R_{\rm free}$ (0.9% of the data) of 29.3 and 29.7%, respectively. As the refinement process proceeded, the corresponding atoms of the oxidized form were added and partial occupancies for both forms fixed at 0.7 reduced and 0.3 oxidized. The two positions for Fe8 and S7 were then added together with the respective conformations for residues 398–402 (Cys399 is directly bound to Fe8 in the reduced form and through a persulfide moiety in the as-isolated oxidized form) and Glu487 (directly bound to Fe8 in both forms) with the same relative occupancies. Finally, the various O atoms in the two forms of the protein were also included. Since the version of *REFMAC* used did not allow the refinement of occupancies, an independent refinement using *SHELXL* (Sheldrick & Schneider, 1997) was performed in which group occupancies for the reduced and oxidized forms of the cluster were refined (D. Aragão, personal communication). As a consequence, the occupancies were adjusted to 0.65 and 0.35 for the reduced and oxidized form of the cluster, respectively, in the final cycles of the *REFMAC* refinement. This resulted in a better agreement between the temperature factors of equivalent atoms in the two forms of the hybrid cluster. Nevertheless, some individual adjustments were made for the O atoms in the oxidized and reduced forms of the protein, as discussed in the next section.

The geometries of the cluster atoms were unrestrained throughout the refinement and in the final stages all the Fe and S atoms (inorganic S and cysteine S) associated with the cubane cluster in each molecule were allowed to refine anisotropically. After the first round of refinement, solvent molecules were added to the model based on standard geometrical and chemical restraints; they were subsequently deleted if their isotropic thermal coefficients exceeded 45 $Å^2$ or if they were not visible at the 0.8 r.m.s. level in σ_A-weighted $|F_o| - |F_c|$ electron-density maps. In several regions, solvent molecules were close together, indicating either partially occupied sites or possible stretches of polyethylene glycol density. As far as possible, where solvent peaks occurred within 2.0 Å of one another, they were treated as partially occupied sites with occupancies (not refined) roughly proportional to the peak volumes. In addition to the solvent peaks assigned to water, there are two regions of density that are clearly different from the normal solvent structure. The first of these lies in the vicinity of the cubane cluster in molecule *A* and was tentatively assigned as a dithionite anion (DTN) in the reduced structure (Aragão *et al.*, 2003), since

Table 2
Refinement statistics.

Amino acids	2 × 544
Protein atoms	4195 (*A*), 4205 (*B*)
Solvent atoms	1645
No. in dual conformations	29
Other atoms	2 cubane and hybrid clusters + 1 MES
Resolution limits (Å)	27.52–1.25
R (all data)	0.140 (227130)
Test set *R* (observations)	0.153 (2141)
Highest resolution shell (1.29–1.25 Å)	
R (working set)	0.206 (13493)
Free *R* (test set)	0.221 (125)
ESU based on maximum likelihood (Å)	0.026
Average B_{iso} (Å^2)	
All atoms (10138)	11.6
Protein atoms	8.8 (*A*), 9.0 (*B*)
Main chain	7.9 (*A*), 8.1 (*B*)
Side chain	9.7 (*A*), 10.0 (*B*)
Solvent	25.1
Residues not found	Gly544 (*A* and *B*)
Residues in alternative conformations (residues in bold type are linked to Fe8)	*A*: V21, R61, M90, S101, K165, N168, M174, S345, I347, E364, **G398**, **C399**, **D400**, **G401**, **R402**, E414, N436, **E487**. *B*: V21, Q46, D59, K165, E167, M174, K250, K290, V302, I338, E340, S345, N436, **G398**, **C399**, **D400**, **G401**, **R402**, N436, S455, I483, **E487**, I529.
Distance deviations†	
Bond distances (Å)	0.008
Bond angles (°)	1.351
Planar groups (Å)	0.005
Chiral volume deviation (Å^3)	0.147

† R.m.s. deviations from standard values.

Table 3
Quality of reduced HCP structures.

G factor and Ramachandran analysis (Ramakrishnan & Ramachandran, 1965) were determined using *PROCHECK* (Laskowski *et al.*, 1993).

Overall *G* factor	0.21
Ramachandran analysis (%) (No. of residues)	
Favourable	93.6 (887)
Additional	5.7 (54)
Generous	0.3 (3)
Disallowed†	0.4 (4)
No. of glycine residues	2 × 49
No. of proline residues	2 × 18

† The residues in the disallowed region of the Ramachandran plot, Ser263 and Asn299 in both molecules *A* and *B*, lie in well defined regions of electron density at sharp bends between helices and strands.

dithionite was used in the protein-reduction process. In the current structure it has been modelled by two water molecules (W1182 and W1334), both occupying two positions. The density does not appear to be present near the cubane cluster in molecule *B*. The second region of density lies between molecules *A* and *B* in the asymmetric unit and can clearly be ascribed to an MES molecule; 0.1 *M* MES buffer was used in the crystallization process. One of the sulfite O atoms interacts with the side chain of Lys313 in molecule *B*. A second interacts with the main-chain amino atom of Asp314, also in molecule *B*, and with a neighbouring solvent molecule, whilst the third interacts with a solvent molecule only. The morpholino moiety fits into a pocket in molecule *A* in the vicinity of Lys434.

For the protein, H atoms were included as 'riding' atoms. Details of the final refinement statistics are given in Tables 2 and 3. Several residues were modelled in more than one conformation. A number of the surface-residue side chains, particularly lysines, had no visible electron density after the CG atom, but as far as possible these were modelled in geometrically feasible positions. Details are shown in Table 2.

3. Results and discussion

The HCPs from the sulfate-reducing bacteria *D. desulfuricans* ATCC27774 and *D. vulgaris* (strain Hildenborough) have three domains as shown in Fig. 2. The N-terminal domain, residues 1–220, comprises two three-helix bundles arranged perpendicular to one another as shown on the right-hand side of Fig. 2. The first 21 residues encompass a standard [4Fe–4S] cluster which is readily accessible to the external environment and may play a role in electron transfer. Each of the second and third domains consists of a central β-sheet with helices above and below as indicated in the top left and bottom left of Fig. 2, respectively. The hybrid cluster lies at the interface of the three domains and is some 11–12 Å distant from the cubane cluster. In the as-isolated oxidized form, whether the protein is isolated aerobically or anaerobically (Macedo *et al.*, 2002), the hybrid cluster can be considered as being derived from a cube, but with an Fe atom, Fe7, at one corner peeled back as shown in Fig. 3(*a*) (Macedo *et al.*, 2002). The hybrid cluster contains both μ-S and μ-O bridges between pairs of Fe atoms. Thus, O8 and O9 bridge Fe6 and Fe8, and bridge Fe7 and Fe8, respectively. A further moiety, *X*, appears to bridge

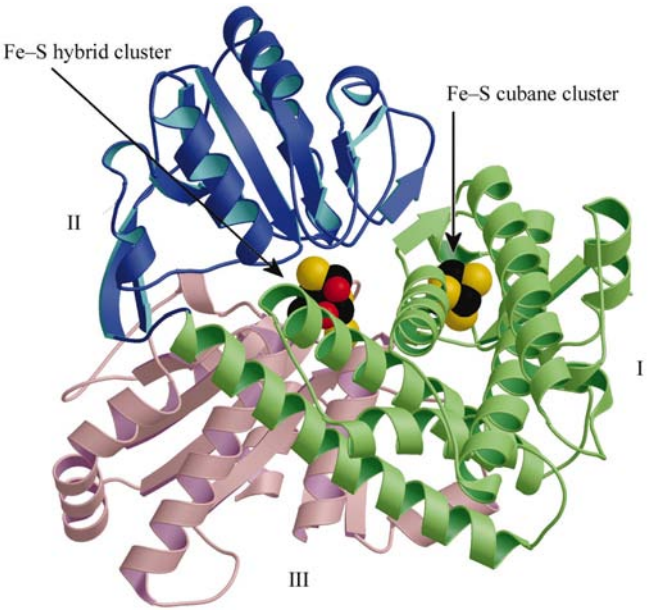

Figure 2
An overall view of the hybrid cluster protein showing the three domains and the two Fe–S clusters: a cubane cluster situated near the outside of the protein in the vicinity of the N-terminus in domain 1 and the hybrid cluster at the interface of the three domains.

Fe5 and Fe7 and in this case the environments of the Fe atoms can be described as distorted tetrahedral for Fe5 and Fe6 and distorted trigonal bipyramidal for Fe7. The coordination of Fe8 is distorted trigonal bipyramidal, but if *X* is also considered it becomes distorted octahedral. In the as-isolated oxidized form of the protein, *X* has been assigned as an O atom, O11.

In the reduced form (Aragão *et al.*, 2003; Fig. 3*b*), the overall molecular structure is virtually the same, but there are major changes at the hybrid cluster. As shown in Fig. 3(*c*), a superposition of the oxidized and reduced forms, the Fe7 atom linked to the protein through residues His240, Glu264 and Cys452 is virtually unchanged in position. The [2Fe–2S] moiety involving Fe5 and Fe6 and linked to the protein through cysteine residues 427 and 308, respectively, undergoes a small movement, but Fe8 and S7 of the persulfide moiety at Cys399 undergo large movements in position and coordination. Concomitantly, residues 398 to 402, including Cys399, and Glu487 attached to Fe8 also undergo significant positional changes. In the reduced form the atom S7 is close to the position of the moiety *X* in the oxidized form, so that it forms the second side of a cube in conjunction with atoms Fe5, Fe8 and S6 and is only 2.4 Å from Fe7; the SG of Cys399 is directly bonded to Fe8. As the protein is oxidized, S7 moves by some 3.6 Å in *Dd* to from a persulfide group with Cys399 and forms a direct bond with Fe8 (Fig. 3*a*). In turn, Fe8 moves by some 2.1 Å in *Dd* between the reduced and oxidized forms. The geometries of the Fe atoms in the reduced form of the hybrid cluster can now be described as tetrahedral for Fe5, Fe7 and Fe8 and trigonal planar for Fe6, in sharp contrast to those observed in the as-isolated oxidized cluster. The hybrid cluster in the reduced form of the protein also lacks the μ-bridging O atoms O8 and O9 between Fe6 and Fe8, and between Fe7 and Fe8, respectively, present in the as-isolated form. However, there appears to be a moiety binding at *Y*, not present in the as-isolated form and roughly in between the positions formerly occupied by O8 and O9. *Y* has currently been assigned as a single O atom (O12), but it could be a larger moiety. *Y* is some 3.1 and 3.4 Å from Fe7 and Fe8, respectively, which is too long for a direct bond. It is, however, well within hydrogen-bonding range of Lys48 NZ9 (2.9 Å) and Asn307 ND2 (3.1 Å); both these residues are conserved in most of the known HCP sequences.

In the present structure both the as-isolated and reduced forms of the HCP appear to be present in the crystal. This is clearly illustrated in Fig. 4, which shows electron density corresponding to the two forms individually and combined. It is not clear how this has occurred since the protein was prepared anaerobically in the as-isolated oxidized state and no deliberate attempts to reduce it were made. Radiation damage

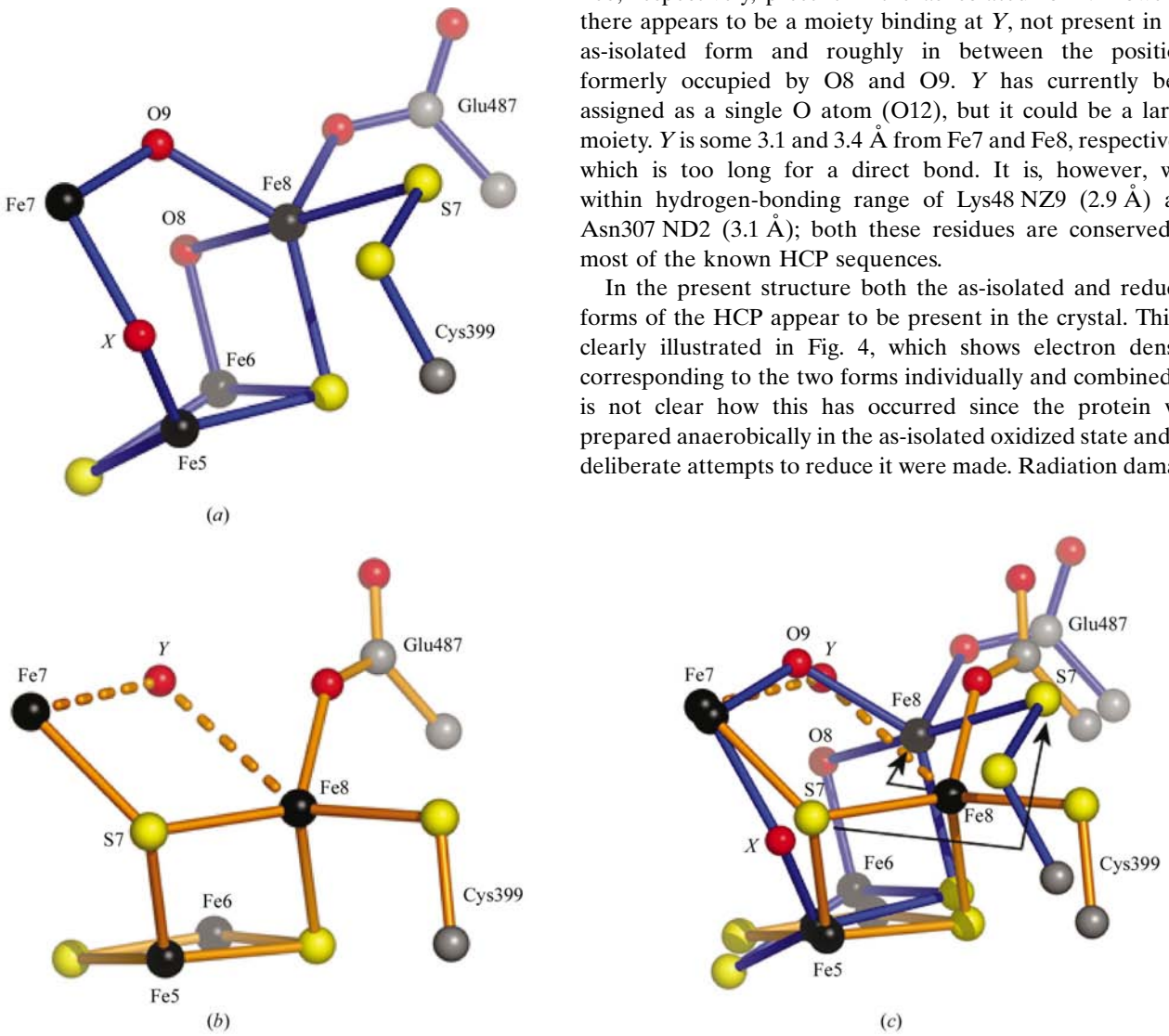

Figure 3
Models of the as-isolated oxidized (*a*) and reduced (*b*) forms of the hybrid cluster. In (*c*) the two forms of the protein have been superimposed and the movements of Fe8 and S7 from the reduced to the oxidized form are marked with arrows. The large movements of Fe8 and S7 and the loss of the bridging O atoms can be clearly envisaged. The ligands bound to Fe5, Fe6 and Fe7 have been omitted for clarity in all three figures, as have Asn307 and Lys489, which may form hydrogen bonds with *Y* in the reduced structure in (*b*).

is known to cause reduction, but a close examination of the data gave no clear evidence that radiation damage was significant. The reduction has presumably occurred as a result of transportation between continents and/or prolonged storage! A model with 65 and 35% of the reduced and oxidized structures explains most of the electron density in σ_A-weighted $2|F_o| - |F_c|$ and $|F_o| - |F_c|$ electron-density maps at the hybrid clusters with the exception of that in the vicinity of the O8 and O9 atoms in the oxidized and the O12 atom in the reduced structure. Increasing the occupancies of O8 and O9 and decreasing the occupancy of O12 alleviates any discrepancies, but whether such adjustments have any experimental significance is debatable. If they are real, then they may indicate that the crystal also includes some structures intermediate between the as-isolated oxidized and reduced states.

In a previous paper (Aragão *et al.*, 2003), a reductase enzyme mechanism was proposed in which the substrate initially binds to the reduced form of the enzyme close to the position of *Y* (O12) (Fig. 3*b*). Reduction of the substrate, with concomitant oxidation of the enzyme, will then take place as the substrate moves from the *Y* position to the *X* (O11) position in the as-isolated oxidized form (Fig. 3*a*). The product will then diffuse away from the active site through the extensive hydrophobic cavity that gives ready access to the hybrid cluster (Cooper *et al.*, 2000) and eventually away from the enzyme. The large movement of S7 makes the *X* position accessible in the oxidized form of the enzyme and may have some role in the substrate movement and its reduction by electron transfer. As a consequence of the translocation of the substrate and its reduction, two O atoms are introduced into the cluster at O8 and O9. Whether these arise from one or more substrate molecules and/or are derived from solvent molecules is not yet known. However, an oxidase activity for the HCP proteins cannot be discounted at this stage. In this case, the substrate would initially bind at *X* in the as-isolated

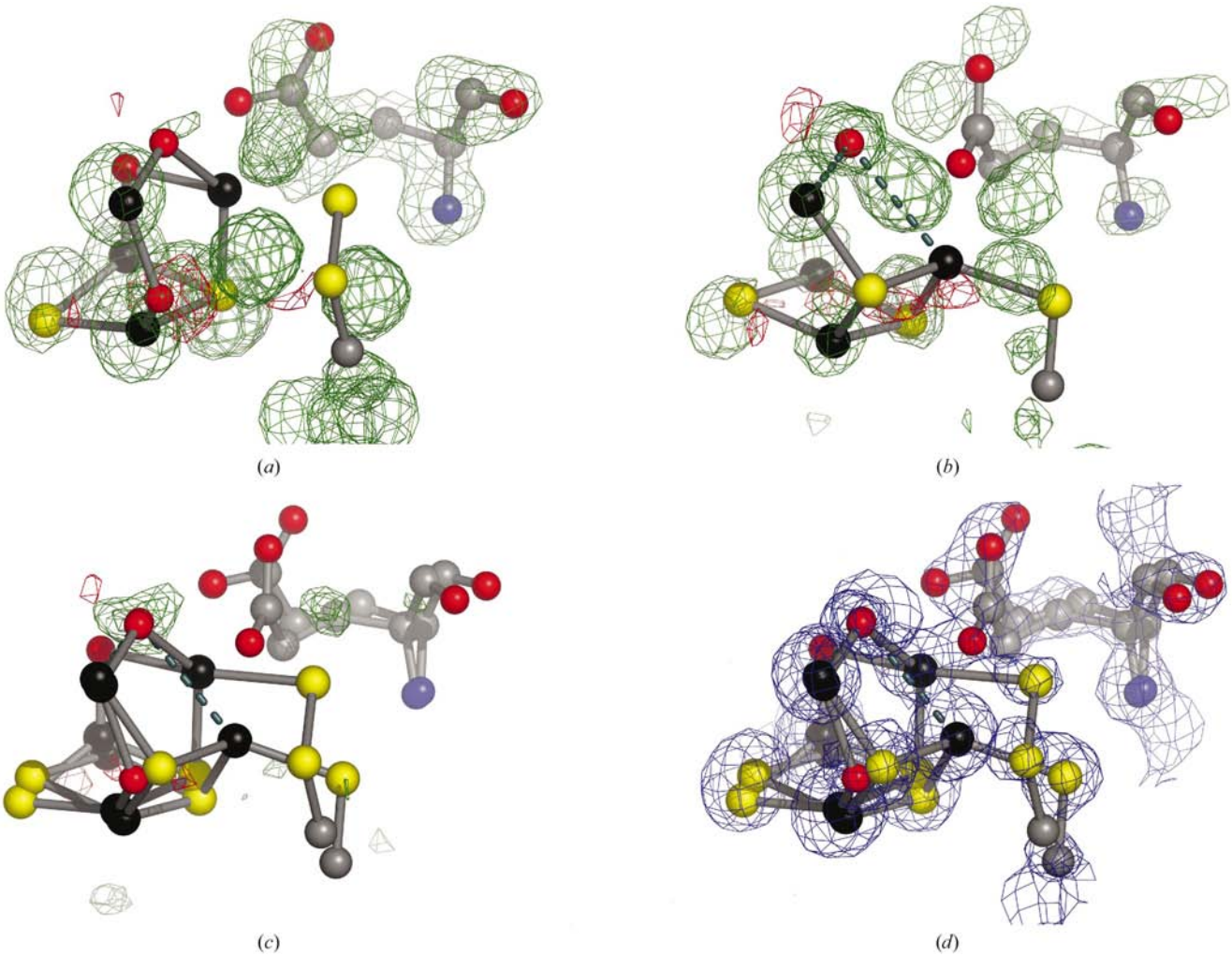

Figure 4
σ_A-weighted electron-density syntheses showing the presence of the as-isolated oxidized and reduced forms of the HCP in the vicinity of the hybrid cluster. In (*a*), (*b*) and (*c*) the Fourier coefficients used were $|F_o| - |F_c|$ and phases were based on (*a*) the as-isolated oxidized form, (*b*) the reduced form and (*c*) both forms in the ratio 65% reduced to 35% oxidized; the contour levels are +3.5 r.m.s. (green) and −3.5 r.m.s. (red). The only feature of chemical interest in (*c*) is a peak at 4–5 r.m.s. close to O9 in the oxidized form and *Y* (O12) in the reduced form. This peak may correspond to a partial substrate or product (see §3). (*d*) is the same as (*c*) but with $2|F_o| - |F_c|$ coefficients; the contour level is 1.0 r.m.s. (blue).

oxidized form of the enzyme and then translocate to *Y*, gaining one of more O atoms from O8 and O9 as the enzyme is reduced. Until the nature of *X* and *Y* are clarified, the function of the HCPs will remain undefined.

Studies on the HCP proteins enable a number of observations to be made. Firstly, the adage that it is highly desirable to use freshly prepared protein for crystallization studies appears to be strongly reinforced. Secondly, crystallographic studies alone, even if they are derived from high-quality high-resolution data, cannot always precisely define what function an enzyme performs or indeed how it achieves this function. Proteomics specialists beware! In this case, even with extensive biochemical and spectroscopic studies, the nature of *X* and *Y* and the meaning of the changes observed in the structure of the hybrid cluster as it transforms between the reduced and oxidized states remain to be determined, although they may give strong credence to the role of the HCPs as reductases. What is clearly indicated by the structural changes in the HCPs in moving between the reduced and the oxidized state and *vice versa*, concomitantly with the large movements of Fe8 and S7, is that they involve a gain or loss, respectively, of the two bridging O atoms O8 and O9. In the former case, this would indeed be consistent with the sequestration of oxygen and/or its byproducts (eventually together with reactive nitrogen species) in an anaerobic environment. That is, the HCP could protect the organisms against oxidative stress (Briolat & Reysset, 2002) or against reactive nitrogen species. As the enzyme returns to its reduced state the O atoms would be released as two water molecules.

Clearly, additional studies are required and further biochemical, spectroscopic and crystallographic studies are in progress to attempt to define the function of the HCPs and to examine the hypotheses mentioned above.

We thank the European Synchrotron Radiation Facility, Grenoble, France and the staff of Macromolecular Crystallography Group for the provision of synchrotron-radiation facilities without which the high-resolution studies would not have been possible. The ESRF also provided a PhD studentship for SM and kindly provided partial support for DGA. DGA acknowledges a grant from Fundação para a Ciência e Tecnologia (FCT), SFRH (BD/6480/2001). We would also like to acknowledge our colleagues at ITQB, M^{a} Armenia Carrondo, Miguel Teixeira, Ligia Saraiva and Carlos Frazão for helpful advice, and the late Jean LeGall and his colleagues in the USA for providing the sample of the HCP protein. PFL would like to acknowledge the assistance and cooperation of the Department of Crystallography, Birkbeck College, University of London, UK. This work was partially funded by FCT, SAPIENS (POCTI/BME/38859/2001). Figures were produced with the help of the programs *Raster3D* (Merritt & Bacon, 1997) and *PyMOL* (DeLano, 2002).

References

Aragão, D., Macedo, S., Mitchell, E. P., Romão, C. V., Liu, M. Y., Frazão, C., Saraiva, L. M., Xavier, A. V., JeGall, J., van Dongen, W. M. A. M., Hagen, W. R., Teixeira, M., Carrondo, M. A. & Lindley, P. (2003). *J. Biol. Inorg. Chem.* **8**, 540–548.

Arendsen, A. F. *et al.* (1998). *J. Biol. Inorg. Chem.* **3**, 81–95.

Beliaev, A. S., Thompson, D. K., Khare, T., Lim, H., Brandt, C. C., Li, G., Murray, A. E., Heidelberg, J. F., Giometti, C. S., Yates, J. III, Nealson, K. H., Tiedje, J. M. & Zhou, J. (2002). *OMICS*, **6**, 39–60.

Berg, W. A. M. van den, Hagen, W. R. & van Dongen, W. M. A. M. (2000). *Eur. J. Biochem.* **267**, 666–676.

Briolat, V. & Reysset, G. (2002). *J. Bacteriol.* **184**, 2333–2343.

Collaborative Computational Project, Number 4 (1994). *Acta Cryst.* D**50**, 760–763.

Cooper, S. J., Garner, C. D., Hagen, W. R., Lindley, P. F. & Bailey, S. (2000). *Biochemistry*, **39**, 15044–15054.

Cowtan, K. D. & Main, P. (1998). *Acta Cryst.* D**54**, 487–493.

DeLano, W. L. (2002). *The PyMOL Molecular Graphics System*. DeLano Scientific, San Carlos CA, USA. http://www.pymol.org.

Dobbek, H., Svetlitchnyi, V., Gremer, L., Huber, R. & Meyer, O. (2001). *Science*, **293**, 1281–1285.

Jones, T. A., Zou, J. Y., Cowan, S. W. & Kjeldgaard, M. (1991). *Acta Cryst.* A**47**, 110–119.

Kim, C. C., Monack, D & Falkow, S. (2003). *Infect. Immun.* **71**, 3196–3205.

Laskowski, R. A., MacArthur, M. W., Moss, D. S. & Thornton, J. M. (1993). *J. Appl Cryst.* **26**, 283–291.

Macedo, S., Mitchell, E. P., Romão, C. V., Cooper, S. J., Coelho, R., Liu, M. Y., Xavier, A. V., LeGall, J., Bailey, S., Garner, C. D., Hagen, W. R., Teixeira, M., Carrondo, M. A. & Lindley, P. F. (2002). *J. Biol. Inorg. Chem.* **7**, 514–525.

Matthews, B. W. (1968). *J. Mol. Biol.* **33**, 491–497.

Merritt, E. A. & Bacon, D. J. (1997). *Methods Enzymol.* **277**, 505–524.

Murshudov, G. N., Vagin, A. A. & Dodson, E. J. (1997). *Acta Cryst.* D**53**, 240–255.

Navaza, J. (1993). *Acta Cryst.* D**49**, 588–591.

Otwinowski, Z. & Minor, W. (1997). *Methods Enzymol.* **276**, 307–326.

Ramakrishnan, C. & Ramachandran, G. N. (1965). *Biophys. J.* **5**, 909–933.

Read, R. J. (1986). *Acta Cryst.* A**42**, 140–149.

Sheldrick, G. M. & Schneider, T. R. (1997). *Methods Enzymol.* **277**, 319–343.

Tronrud, D. (1996). *Proceedings of the CCP4 Study Weekend. Macromolecular Refinement*, edited by E. Dodson, M. Moore, A. Ralph & S. Bailey, pp. 1–10. Warrington: Daresbury Laboratory.

Vocht, M. L. de, de Kooter, I. M., Bulsink, Y. B. M., Hagen, W. R. & Johnson, M. K. (1996). *J. Am. Chem. Soc.* **118**, 2766–2767.

Wolfe, M. T., Heo, J., Garavelli, J. S. & Ludden, P. W. (2002). *J. Bacteriol.* **184**, 5898–5902.